

The Cartilaginous Tissue Formation using Sry (Sex Determining Region Y)-BOX9 and Telomerase Reverse Transcriptase Genes Transfected Chondrocytes: *In vivo* Approach

(Pembentukan Tisu Tulang Rawan menggunakan Sry (Penentu Jantina Rantau Y)-BOX9 dan Telomerase Gen Transkripsi Berbalik Kondrosit Transfeksi: Pendekatan *in vivo*)

NOORHIDAYAH MD NAZIR, AHMAD HAFIZ ZULKIFLY, KAMARUL ARIFFIN KHALID, ISMAIL ZAINOL, ZAITUNNATAKHIN ZAMLI & MUNIRAH SHA'BAN*

ABSTRACT

The shortage of organ supply reduces the success rate of organ transplantation. Hence, tissue regeneration has been initiated with the intention of improving the available treatment modalities. Articular cartilage is a suitable tissue for this purpose due to its limited self-heal ability. This study aims to evaluate the cartilaginous properties of in vivo constructs formed using chondrocytes transfected with the combination of sry (sex determining region y)-box9 (SOX9) and telomerase reverse transcriptase (TERT) genes (SOX9/TERT-transfected chondrocytes) seeded on a three-dimensional (3D) poly(lactic-co-glycolic) acid (PLGA)-based scaffold. The rabbit's articular chondrocytes (n=6) were transfected with SOX9 and TERT genes via lipofection. The non-transfected chondrocyte (NTC) was used as a control. A total of 1×10^5 cells were seeded on a PLGA and PLGA/fibrin hybrid scaffolds to form constructs. The resulted constructs were SOX9/TERT-PLGA/fibrin, NTC-PLGA/fibrin, SOX9/TERT-PLGA and, NTC-PLGA. All constructs were cultured for three weeks prior to subcutaneous implantation into the athymic mice for two and four weeks. The constructs' structural and functional aspects were evaluated using macroscopic observation, compression-stress analysis, histology, quantitative sulphated glycosaminoglycan (sGAG) assay and cartilage-specific genes (ACAN, COL2A1, SOX9), TERT, and MMP13 expression analysis. The constructs demonstrated a cartilage-like appearance. The constructs' rigidity corresponded to the homogenous cells and extracellular matrix distribution in the week-4 constructs. Correspondingly, the cartilaginous matrix components were visualised at the pericellular matrix region of the construct, supported by the increment of quantitative sGAG content. The SOX9/TERT-PLGA/fibrin exhibited better genes expression and cartilaginous phenotypes than the other construct groups. The SOX9/TERT-PLGA/fibrin construct facilitated cartilaginous tissue formation.

Keywords: Cartilage; chondrocytes; in vivo; SOX9; TERT; transfection

ABSTRAK

Kekurangan bekalan organ menurunkan kadar kejayaan pemindahan organ. Oleh itu, penjana semula tisu telah diusahakan bagi memperbaiki modaliti rawatan sedia ada. Rawan artikular ialah tisu yang sesuai untuk kegunaan ini oleh sebab kebolehan swapulihnya yang terbatas. Kajian ini bertujuan untuk menilai ciri-ciri tulang rawan binaan in vivo yang dibentuk melalui transfeksi gabungan gen sry (penentu jantina rantau y)-box9 (SOX9) dan gen telomerase transkriptase membalik (TERT) ke dalam sel kondrosit yang disemai atas kerangka tiga dimensi (3D) berasaskan asid poli(laktik-ko-glikolik) (PLGA). Sel kondrosit artikular arnab (n=6) telah ditransfeksi dengan gen SOX9 dan TERT melalui kaedah lipofeksi. Sel kondrosit tanpa transfeksi (NTC) telah digunakan sebagai kawalan. Sejumlah 1×10^5 sel telah disemai atas kerangka PLGA 3D dan kerangka hibrid PLGA/fibrin untuk membentuk binaan. Binaan yang terhasil ialah SOX9/TERT-PLGA/fibrin, NTC-PLGA/fibrin, SOX9/TERT-PLGA dan NTC-PLGA. Semua binaan telah dikultur selama tiga minggu sebelum diimplantasi secara subkutaneus ke dalam tikus tanpa timus selama dua dan empat minggu. Aspek struktur dan fungsian binaan telah dinilai menggunakan pemerhatian makroskopik, analisis tegasan mampatan, histologi, asai kuantitatif glikosaminoglikan sulfat (sGAG) dan analisis ekspresi gen khusus tulang rawan (ACAN, COL2A1, SOX9), TERT dan MMP13. Binaan menunjukkan rupa tulang rawan. Ketegaran binaan sejajar dengan taburan sel homogen dan matriks ekstrasel pada binaan minggu ke-4. Komponen matriks tulang rawan telah dilihat pada binaan di bahagian matriks periselular, disokong oleh kenaikan kandungan kuantitatif sGAG. SOX9/TERT-PLGA/fibrin mempamerkan ekspresi gen dan fenotip tulang rawan yang lebih baik berbanding kumpulan binaan yang lain. Binaan SOX9/TERT-PLGA/fibrin memudahkan pembentukan tisu tulang rawan.

Kata kunci: In vivo; sel kondrosit; SOX9; TERT; transfeksi; tulang rawan

INTRODUCTION

The establishment of cell culture helps the researchers to study the cells' behaviour. A recognised cartilage repair treatment modality, autologous chondrocyte implantation (ACI) applies cell culture technique using the retrieved chondrocytes from the damaged cartilage site (Ogura et al. 2019). The cultured chondrocytes are implanted to the site with the hope that new tissue will grow at the defected area. However, the fate of the implanted cell is unknown because it has been indicated that the cultured chondrocytes tend to dedifferentiate in monolayer culture (Kavand et al. 2019; Mohd Yunus et al. 2019; Vermeulen et al. 2019).

The introduction of tissue engineering and regenerative medicine (TERM) gives hope to improve the existing medical intervention, particularly for treating cartilage damage. In TERM, tissue regeneration is achieved by incorporating the cells into the 3D scaffold with the supplementation of signalling cues. Hence, the 3D culture setting is expected to provide a better implant quality than the monolayer culture because the cultured cells are developing towards functioning tissue (Prosser et al. 2019). It shows the importance of cells interaction in the scaffold as the formed construct mimics the tissue in its actual condition, that is in the form of multicellular layers. Several cartilage TERM studies have demonstrated cartilaginous phenotype restoration in the *in vitro* cultured construct (Kudva et al. 2018; Liu et al. 2019; Elakkiya et al. 2019). Hence, the confirmation of tissue development in the *in vitro* construct has to be analysed in the *in vivo* setting, as it is close to an actual environment. For instance, it has been reported that the implanted construct in an ectopic animal model (athymic mice) has exhibited positive tissue growth in just four weeks (Deng et al. 2019; Joydip et al. 2013), six weeks (Zhang et al. 2019), seven weeks (Zhu et al. 2014) chondrocytes can maintain stable chondrogenic phenotype in ectopic microenvironment, which was speculated to be related with the existence of anti-angiogenic factors such as Chondromodulin-I (Chm-I and eight weeks (Sabatino et al. 2012) post-implantation.

In this study, the construct is formed by seeding the chondrocytes transfected with *SOX9* and *TERT* genes (*SOX9/TERT*-transfected chondrocytes) in PLGA/fibrin and PLGA scaffolds. *SOX9* is the chondrogenesis master regulator which activates other cartilaginous markers, namely collagen type-II and aggrecan and suppresses hypertrophy marker, collagen type-X in non-hypertrophic chondrocytes (Zhang et al. 2017). In the case of *TERT*, it is anticipated to delay the apoptosis or senescence of the cells. The potential of *SOX9/TERT*-transfected chondrocytes has been verified in the *ex vivo* experimental setting (Noorhidayah et al. 2019). The finding has demonstrated the formation of cartilaginous tissue with a stable phenotypic expression in the construct that has been formed using *SOX9/TERT*-transfected chondrocytes compared to the other cell groups. However, the tissue's

histoarchitecture has not fully occupied or infiltrated into the porous scaffold. As a continuation of the report, this study aims to evaluate the constructs' performance in the *in vivo* environment.

MATERIALS AND METHODS

CHONDROCYTES ISOLATION

With the approval of the Institutional Animal Care and Use Committee, International Islamic University Malaysia (IACUC-IIUM) (IIUM/IACUC/Approval 2015/[5]/[24]), the 6-months old New Zealand White rabbits (n=6) were obtained from a commercially available source in Kuantan, Pahang. Articular cartilage was aseptically harvested from the femoral condyle and tibial plateau. The chondrocytes isolation procedure was conducted as described in Noorhidayah et al. (2019). The cultured cells were supplemented with 1:1 of Ham's F12 nutrient mixture (F12) and Dulbecco's Modified Eagles Medium (DMEM) culture medium supplemented with 1% (v/v) AA (Gibco, Grand Island, NY), 10% (v/v) Fetal Bovine Serum (FBS) (Gibco, Grand Island, NY), 1% (v/v) GlutaMAX™ (Gibco, Grand Island, NY), 1% (v/v) 4-(2-hydroxyethyl)-1-piperazineethanesulfonic acid (HEPES) buffer (Gibco, Grand Island, NY) and 1% (v/v) 50 µg/mL of ascorbic acid (Sigma-Aldrich, St. Louis, Missouri, USA). The cultures were maintained in a 5% CO₂ incubator (Thermo Scientific, Barnstead Lab Line, USA) at 37 °C. The cells were sub-cultured to passage-1 (P1) once it reached 70%-90% confluency.

SOX9 AND TERT GENES TRANSFECTION

The P1 cells were transfected with pcDNA3-*SOX9* and/or pBabe-neo-*hTERT* plasmids via lipofection (Lipofectamine™ 3000, Invitrogen, CA, USA) by following the manufacturer's protocol (Noorhidayah et al. 2019). The procedure managed to achieve the transfection efficiency of 60.38% (unpublished data). The cells were grouped into (a) non-transfected chondrocytes (NTC, control) and (b) *SOX9/TERT*-transfected chondrocytes. The cells were detached from the culture plate with Trypsin-ethylenediaminetetraacetic acid (EDTA) (Gibco, Grand Island, NY, USA) after 24 h and were seeded in the scaffold.

FORMATION OF 3D CONSTRUCT

The disc-shaped (3 mm height × 7 mm diameter) 20% (w/v) PLGA (mole ratio: 65:35, Resomer RG653H, Sigma-Aldrich, St. Louis, Missouri, USA) scaffold with the pore size of 180 µm-250 µm, 85.2% porosity was fabricated using solvent casting and salt leaching technique (Munirah et al. 2008a; Noorhidayah et al. 2019). The *SOX9/TERT*-transfected chondrocytes and NTC at P1 were seeded into a sterilised PLGA scaffold with and without rabbit's plasma-derived fibrin with the concentration of 865,800 cell/cm³ (100,000 cells per 7

mm × 3 mm scaffold) (Table 1). The cells seeded in the PLGA with 250 µL fibrin was coagulated by adding 50 µL calcium chloride (CaCl₂) (Sigma-Aldrich, St. Louis,

Missouri, USA). The formed constructs were cultured for three weeks *in vitro*.

TABLE 1. The experimental groups and relevant abbreviations

Scaffolds		Cells Source	Abbreviation Used
PLGA and fibrin		<i>SOX9</i> and <i>TERT</i> -transfected chondrocytes	<i>SOX9/TERT</i> -PLGA/fibrin (S/T-P/F)
		Non-transfected chondrocytes	NTC-PLGA/fibrin (C-P/F)
PLGA *without fibrin	seeded with	<i>SOX9</i> and <i>TERT</i> -transfected chondrocytes	<i>SOX9/TERT</i> -PLGA (S/T-P)
		Non-transfected chondrocytes	NTC-PLGA (C-P)

CONSTRUCT IMPLANTATION

The *in vitro* cultured constructs were implanted subcutaneously at the dorsum of 6-week old athymic mice (n= 6). General anaesthesia was carried out with an intramuscular injection of zoletil (25 mg/kg) (Virbac Laboratories, Carros, France) and xylazine (12 mg/kg) (Ilium, Troy Laboratories Pty Limited, Australia) (ZX) cocktail (Choi & Jeong 2017). Under the aseptic condition, four subcutaneous pockets were created per mouse by making a small horizontal incision (approximate of 1 cm) on the dorsum of the mouse's skin. The four pockets were created by manoeuvring a blunt surgical scissor, enough to fit a 7 mm × 3 mm scaffold in the pocket. The construct was carefully inserted in each pocket and sutured with resorbable stitches, 3.0 Vicryl (Johnson & Johnson Healthcare System. Inc., Hoes Lane, Piscataway, New Jersey, USA). The mice were allowed to move freely in an individually ventilated cage (IVC). The *in vivo* constructs were harvested at week-2 and week-4 by overdosing the mice with the ZX cocktail.

MACROSCOPIC OBSERVATION

The constructs were observed at room temperature for its gross appearance, shape, and colour. Simple palpation using forceps was conducted to confirm the construct's rigidity (Alsberg et al. 2002).

COMPRESSION-STRESS ANALYSIS

The analysis was conducted using a biomechanical-testing machine (Instron E300, Oswald Elektromotoren

GmbH, Germany). The construct was stored in normal saline before testing. A constant compressive strain rate of 1 mm/min was applied until failure, and a stress-strain curve was generated. The generated data was used to plot the result.

HISTOLOGICAL STAINING

The construct was fixed in 10% Neutral Buffered Formalin (NBF) (Surgipath®, Leica Microsystem, USA), processed and sectioned to 5 µm. Haematoxylin and eosin (H&E) (Haematoxylin 560MX®, Leica Biosystem Richmond Inc, Canada), alcian blue, pH 2.5 (Merck KGaA, Darmstadt, Germany), toluidine blue, pH 1.0 (Sigma-Aldrich, St. Louis, Missouri, USA) and 0.1% safranin O (Merck KGaA, Darmstadt, Germany) were conducted to observe the structural and functional aspects of the construct.

QUANTITATIVE sGAG ASSAY

The construct was digested in 125 µg/mL papain enzyme (Sigma-Aldrich, St. Louis, Missouri, USA) for 16 h at 60 °C. The sGAG detection was conducted using Alcian Blue assay by following the procedure in Karlsson and Björnsson (2001), as described in Noorhidayah et al. (2019). The absorbance was measured using a VersaMax microplate reader (Molecular Devices, San Jose, California, USA) at 620nm. The data were normalised with the construct's dry weight.

CARTILAGINOUS MARKERS EXPRESSION ANALYSIS
SOX9, aggrecan (*ACAN*) and collagen type-II (*COL2A1*), collagen type-I (*COL1A2*), *TERT* and *MMP13* genes expression were evaluated using real-time polymerase chain reaction (RT-PCR). The primers are listed in Table

2. The reaction was conducted using CFX96 Touch™ Real-Time PCR Detection System (BIO RAD, Hercules, California, USA). The PCR profile for the respective markers are as follows: initial denaturation, 95 °C for 5 min, 39 cycles of 95 °C for 5 s and 60.3 °C for 30 s.

TABLE 2. The used molecular markers primer sequences

Primer's name	Sequences	Accession number	PCR product (bp)
<i>HPRT1</i>	F:5'-GCA GAC CTT GCT TTC CTT GGT-3'	NM_001105671.1	62
	R:5'-GCA GGC TTG CGA CCT TGA C-3'		
<i>COL1A2</i>	F:5'-GGT GGT TAC GAC TTT GGT TA-3'	NM_001195668.1	95
	R:5'-GCA TCG ACT TCA TAG TCC TT-3'		
<i>COL2A1</i>	F:5'-TGC AGG AGG GGA AGA GGT AT-3'	NM_001195671.1	123
	R:5'-GGC AGT CCT TGG TGT CTT CA-3'		
<i>ACAN</i>	F:5'-ACA CTG GCG AGT ACT GTG AC-3'	XM_008251722.2	95
	R:5'-TGT GAA AGA GTC GCT GGC AT-3'		
<i>SOX9</i>	F:5'-AAG ATG ACC GAC GAG CAG GA-3'	XM_008271763.2	116
	R:5'-CGT GTA TTC TCG GTG TCG GA-3'		
<i>TERT</i>	F:5'-TTG CGG AAG ACA GTG GTG AA-3'	NM_198253.2	176
	R:5'-AGA CTG GCT CTG ATG GAG GT-3'		

STATISTICAL ANALYSIS

From the compression-stress analysis, sGAG assay and cartilaginous markers expression, the data were expressed as the mean ± standard error of the mean. The data was tested with the Shapiro-Wilk normality test. Mixed-design ANOVA was used with $p < 0.05$ that was considered statistically significant.

RESULTS AND DISCUSSION

CARTILAGE-LIKE TISSUE MORPHOLOGY

Cartilage TERM approach is perceived as a hope to solve cartilage damage or degeneration issue. A reproducible cartilaginous tissue implant formation is the ultimate goal for any cartilage TERM attempt. Hence, the evaluation of structural and functional aspects of the construct confirmed the construct's potential. In terms of

the construct's macroscopic morphology, the *in vitro* and *in vivo* constructs had retained the disc-shaped structure and were reduced in their diameter as the time point increased (Figure 1). The *in vivo* constructs appeared to have a smoother, glossier surface and were more cartilage-like than the *in vitro* constructs. In addition, no significant difference has been noted between the PLGA/fibrin and PLGA scaffold groups. Based on the resulted construct's morphology, it is possible that the secreted ECM has replaced the degraded biomaterial scaffold and are left with the formed tissue. Besides that, the scaffold size-reduction was perhaps affected by the *in vivo* microenvironment because of its ectopic implantation site. Although it was not implanted at the actual site, this cartilaginous tissue was able to grow under the skin. Hence, it is suggested that the chances of the construct to form cartilaginous tissue in the actual site of implantation may be high.

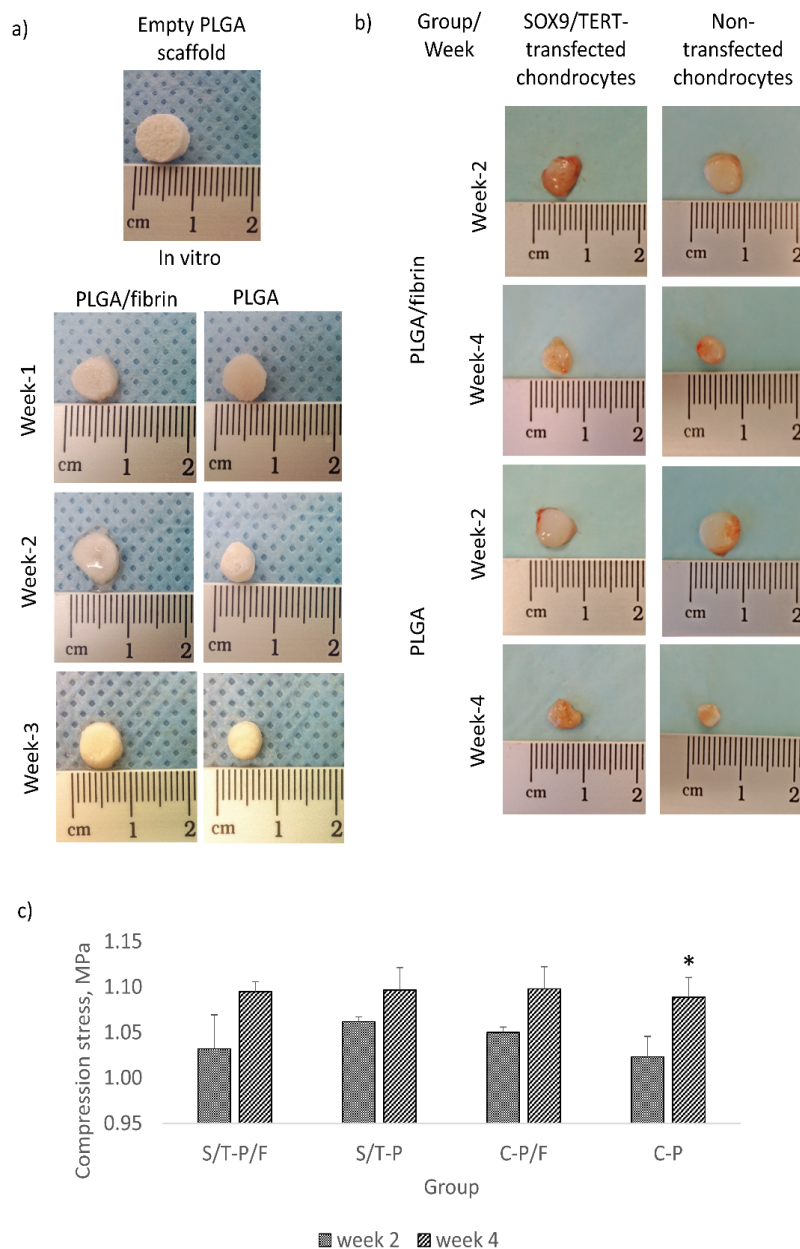


FIGURE 1. a) The representative images of *in vitro* construct gross morphology at week-1, week-2 and week-3, b) The representative images of *in vivo* construct at week-2 and week-4 & c) The mechanical strength of the *in vivo* construct at week-2 and week-4. *represents $p < 0.05$ that is considered as significant. The constructs abbreviation is listed in Table 1

THE INCREMENT OF CONSTRUCT'S RIGIDITY INFLUENCED BY TISSUE'S HISTOARCHITECTURE

A simple palpation test conducted on the *in vivo* construct indicated the increment of the construct's rigidity from week-2 to week-4 post-implantation (Figure 1(c)). The *in vitro* constructs were unable to retain its 3D structure and collapse upon palpation. The post-implanted construct's rigidity outcome was confirmed via compression-stress

analysis. Regardless of scaffold groups, it was noted that the mechanical strength at week-4 of all *in vivo* construct was higher than the construct's strength at week-2. The mechanical strength of the construct groups had increased by 1.06-times, 1.04-times, 1.05-times, 1.07-times in *SOX9/TERT*-PLGA/fibrin, *SOX9/TERT*-PLGA, NTC-PLGA/fibrin, and NTC-PLGA, respectively. There were no significant differences between each week,

$F(1.00,5.00)=4.42$, $p>0.05$. There was also no significant differences between each group, $F(3.00,15.00)=0.91$, $p>0.05$. There was no significant interaction between weeks and groups, $F(3.00,15.00)=0.42$, $p>0.05$.

Based on the result, it is noted that the construct's structure at week-2 is more porous than the construct at week-4 due to the lower mechanical strength value. It is believed that the cells interaction and ECM distribution contribute to the mechanical strength of the *in vivo* constructs (Wang et al. 2016). As supported by the histological visualisation (Figure 2(a)), less-homogenous cells and ECM infiltration had been observed in the construct at week-2, while the week-4 construct structure was wholly occupied with the matrix. From the visualisation, the resulted histoarchitecture of the week-4 construct was comparable with the one that was reported at week-16 post-implantation (Calabrese et al. 2017), indicating the cells dynamic interaction with the *in vivo* environment. While the *in vitro* cartilaginous tissue was formed thinly on the outer part of the scaffold corresponded to the unstable *in vitro* construct structure caused by the incomplete cells and matrix infiltration (Noorhidayah et al. 2019). In addition, there was no significant difference in terms of cartilage histoarchitecture formation in both PLGA/fibrin and PLGA scaffold groups.

THE INCREASE OF CARTILAGINOUS MATRIX COMPONENT PRODUCTION IN THE *IN VIVO* CONSTRUCT

The cartilaginous matrix components (sGAG and proteoglycan) secretion were in its infant state in the *in vivo* construct, even though the construct had exhibited cartilage histoarchitecture formation with distinct chondrocytes morphology in the matrix.

The blue stain of alcian blue representing positive sGAG indicator was visualised at the pericellular matrix region of the *in vivo* and *in vitro* constructs at all designated time points (Figure 2(b)). The sGAG was concentrated at the pericellular matrix region with less-homogenous distribution in the constructs. The distribution of sGAG in the matrix showed that the secretion of sGAG was still in its primitive stage in the *in vivo* construct, indicating that the formed cartilaginous tissue was young. In addition, the intense alcian blue stain in the week-4 constructs was a sign that the formed cartilaginous tissue was progressing towards maturation. The histological outcome was supported by the quantitative sGAG content increment in the *in vivo* construct (Figure 2(c)). The sGAG content had increased by 1.40-times, 1.54-times, 2.55-times, 1.64-times in *SOX9/TERT*-PLGA/fibrin, *SOX9/TERT*-PLGA, NTC-PLGA/fibrin and NTC-PLGA, respectively. There was no significant difference between each week, $F(1.00,5.00)=1.77$, $p>0.05$. There was also no significant difference between each group, $F(3.00,15.00)=1.69$,

$p>0.05$. There was no significant interaction between weeks and groups, $F(3.00,15.00)=0.15$, $p>0.05$. There was an increment of quantitative sGAG content in the *in vitro* constructs (Noorhidayah et al. 2019). It showed that the sGAG had continuously been produced in both the *in vitro* and *in vivo* constructs as the time point increased.

The sGAG production stimulates the presence of proteoglycan in the matrix as it is made up of sGAG chains that are bonded with a core protein. In this study, proteoglycan visualisation through toluidine blue corresponds to the sGAG histological outcome. The dark purple stain of toluidine blue was detected at the pericellular matrix region in the *in vivo* and *in vitro* constructs (Figure 3(a)). As for the proteoglycan detection through safranin O, an intense orange-red stain was displayed in the *in vitro* constructs indicating the presence of proteoglycan-rich matrix. In the *in vivo* constructs, the protein was more visible at the pericellular matrix region of week-4 in the *SOX9/TERT*-PLGA/fibrin compared to the other groups (Figure 3(b)). The low detection of proteoglycan through safranin O is expected due to the stain having a low affinity towards sulphur in the tissue that can only be detected in mature cartilage (Schmitz et al. 2010). From the overall histology visualisation, it can be noted that the *in vivo* construct is a premature cartilaginous tissue.

Besides that, the presence of collagen type-II and collagen type-I were detected in the construct via immunohistochemistry staining (Figure 4). The immunopositivity of collagen type-II was noted in the *in vitro* and *in vivo* constructs with the accumulation of brown precipitation at the pericellular matrix region. Collagen type-II was expressed in all constructs at all designated time points. The collagen's immunoreaction was particularly homogenous in *SOX9/TERT*-PLGA/fibrin compared to other constructs. As for the collagen type-I immunoreaction, the collagen was expressed in the *in vitro* setting. However, the brown precipitation was not visible at the pericellular matrix region in all *in vivo* constructs. Among all the constructs, *SOX9/TERT*-PLGA/fibrin at week-4 had shown prominent negative collagen type-I immunoreaction.

Collagen type-II is a specific marker for hyaline cartilage and only presented in the mature cartilage. Despite that, the co-expression of collagen type-II and collagen type-I is known to be a sign of the developing cartilage (Munirah et al. 2008b; Noorhidayah et al. 2019), which is based on the previous rat tibial articular cartilage development study (Sasano et al. 1996). This event is noted in the 3D culture outcome which highlights the phenotypically immature *in vitro* cartilaginous tissue. Even so, the tissue is progressing towards maturation as the ectopic implanted construct has shown its potential as hyaline cartilage with the non-detected immunopositivity of collagen type-I in the groups.

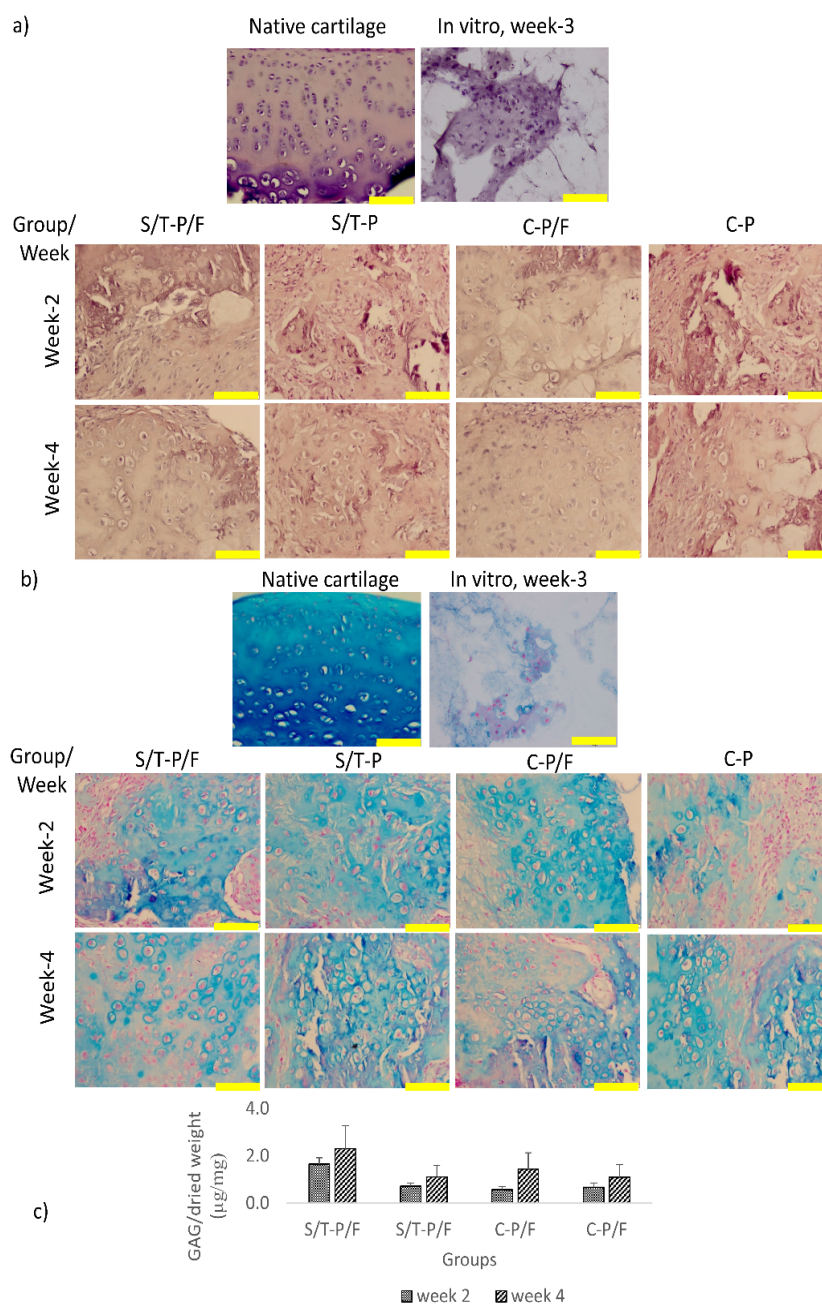


FIGURE 2. a) The images show the morphology or histoarchitecture of the *in vivo* construct that has been stained using haematoxylin and eosin, b) The presence of sGAG at the pericellular matrix region is indicated as the blue stain in the *in vivo* 'construct that has been stained using alcian blue'. Magnification = 200X. Scale bar = 100 µm (yellow coloured) & c) The quantitative sGAG content increment in the *in vivo* construct. *represents $p < 0.05$ that is considered as significant. The constructs abbreviation is listed in Table 1

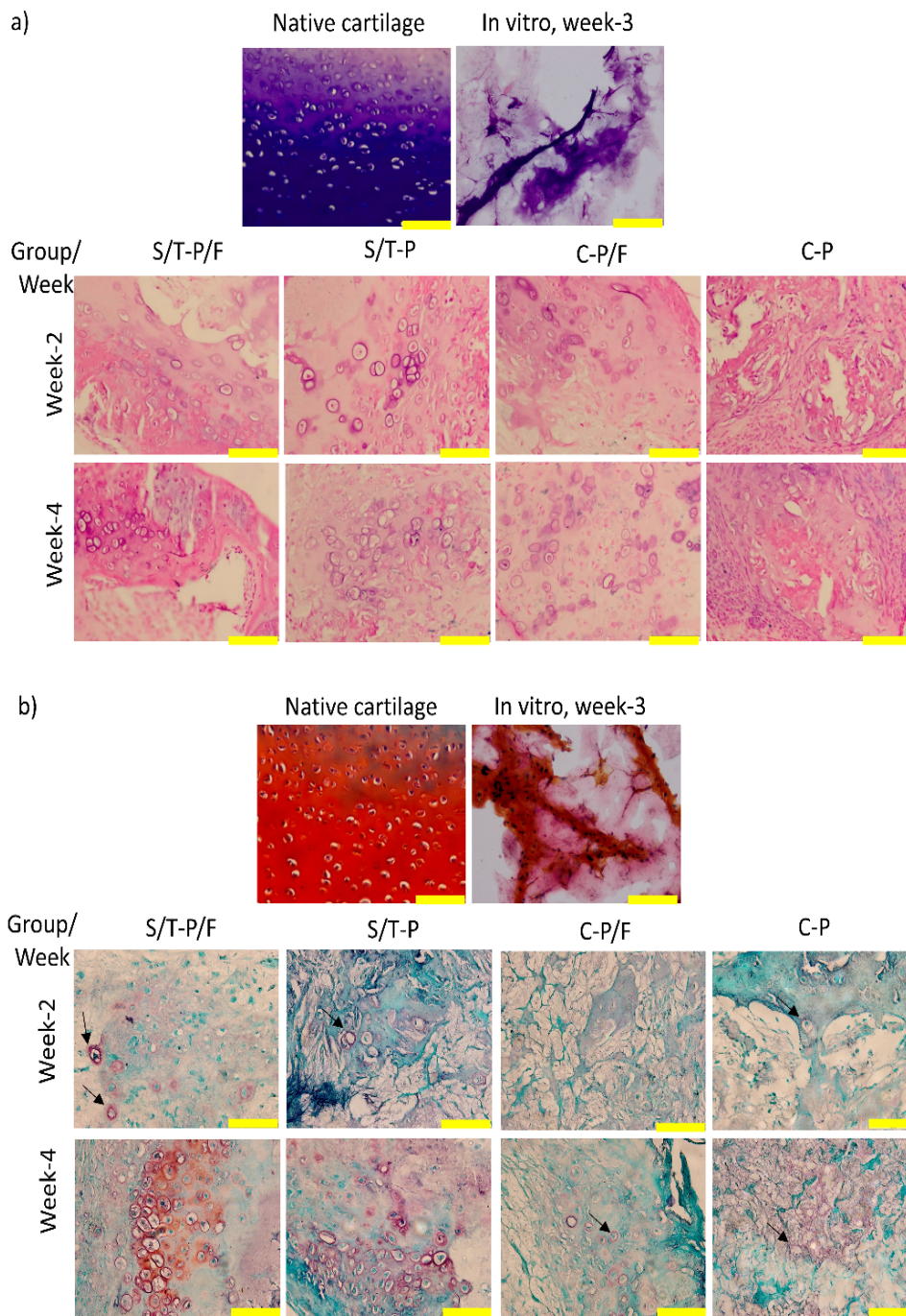


FIGURE 3. a) The presence of proteoglycan at the pericellular matrix region of the *in vivo* construct is indicated as the dark purple stain of toluidine blue & b) The presence of proteoglycan at the pericellular matrix region of the *in vivo* construct is indicated as the orange-red stain of safranin O has been detected, particularly in *SOX9/TERT*-PLGA/fibrin at week-4. The arrows indicate the accumulation of proteoglycan at the pericellular matrix region. Magnification = 200X. Scale bar = 100 μ m (yellow coloured). The constructs abbreviation is listed in Table 1

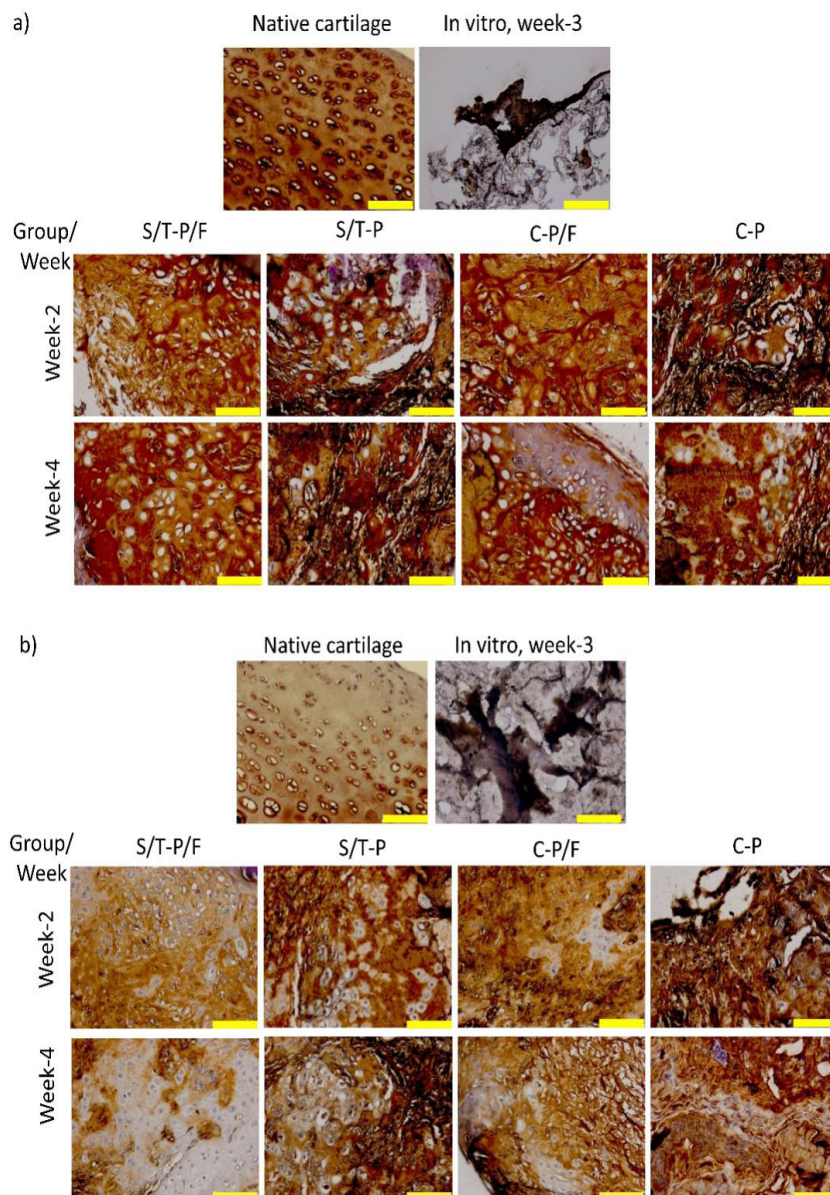


FIGURE 4. a) The brown precipitation indicates the presence of collagen type-II at the pericellular matrix region of the *in vivo* construct using immunohistochemistry & b) The brown precipitation indicates the presence of collagen type-I at the pericellular matrix region of the *in vivo* construct that has not been detected, particularly in *SOX9/TERT*-PLGA/fibrin at week-4. Magnification = 200X. Scale bar = 100 μ m (yellow coloured). The constructs abbreviation is listed in Table 1

THE UPREGULATION OF CARTILAGINOUS MARKERS EXPRESSION IN *SOX9/TERT*-PLGA/FIBRIN CONSTRUCT

The gene expression result demonstrated the upregulation of proteoglycan marker, *ACAN* in the *in vivo* *SOX9/TERT*-PLGA/fibrin construct (Figure 5(a)). The gene expression was upregulated from 1.00 ± 0.51 -fold at week-2 to 3.63 ± 0.58 -fold at week-4 in the construct group, by 3.63-times. The *ACAN* expression result indicates that there was no significant difference between each week, $F(1.00, 5.00) = 0.58$, $p > 0.05$. There was also no significant

difference between each group, $F(3.00, 15.00) = 2.71$, $p > 0.05$. There was no significant interaction between weeks and groups, $F(3.00, 15.00) = 2.71$, $p > 0.05$. The *ACAN* expression level in *SOX9/TERT*-PLGA/fibrin corresponds to the histological visualisation, as the proteoglycan rich-matrix was visibly increased in the construct through safranin O (the mature cartilage detector). In the *in vitro* constructs, the gene expression was also significantly upregulated in the *SOX9/TERT*-PLGA/fibrin (Noorhidayah et al. 2019).

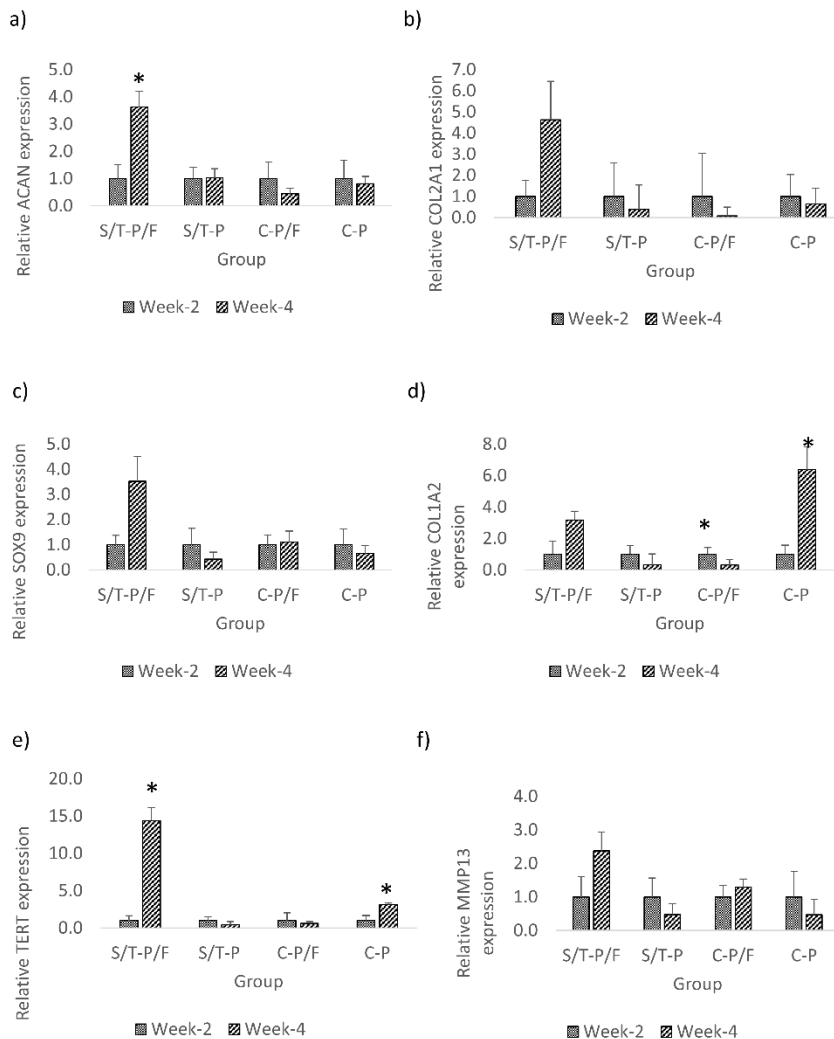


FIGURE 5. a) *ACAN* gene expression was upregulated in the *in vivo* *SOX9/TERT*-PLGA/fibrin, b) *COL2A1* gene expression was upregulated in the *in vivo* *SOX9/TERT*-PLGA/fibrin, c) *SOX9* gene expression was upregulated in the *in vivo* *SOX9/TERT*-PLGA/fibrin and NTC-PLGA, e) *TERT* gene expression was upregulated in the *in vivo* *SOX9/TERT*-PLGA/fibrin and NTC-PLGA & f) *MMP13* gene expression was upregulated in the *in vivo* *SOX9/TERT*-PLGA/fibrin and NTC-PLGA/fibrin. *represents $p < 0.05$ that is considered as significant. The constructs abbreviation is listed in Table 1

Similar with *ACAN* expression the *in vivo* construct, *COL2A1* expression was upregulated in the *SOX9/TERT*-PLGA/fibrin. The upregulation of *COL2A1* gene expression was from 1.00 ± 0.76 -fold at week-2 to 4.63 ± 1.81 -fold at week-4 (Figure 5(b)). There was no significant difference between each week, $F(1.00, 5.00) = 2.48$, $p > 0.05$. There was also no significant difference between each group, $F(1.11, 5.53) = 2.57$, $p > 0.05$. There was no significant interaction between weeks and groups, $F(1.11, 5.53) = 2.57$, $p > 0.05$. The gene was also upregulated in the *in vitro* constructs made of

SOX9/TERT-transfected chondrocytes, which were *SOX9/TERT*-PLGA/fibrin and *SOX9/TERT*-PLGA (Noorhidayah et al. 2019).

The upregulation of *SOX9* gene in the *in vivo* *SOX9/TERT*-PLGA/fibrin was expected as both *ACAN* and *COL2A1* were well-expressed in the construct (Figure 5(c)). *SOX9* gene expression was increased by 3.52-times in the construct group. There was no significant difference between each week, $F(1.00, 5.00) = 0.01$, $p > 0.05$. There was a significant difference between each group, $F(3.00, 15.00) = 4.21$, $p < 0.05$. Among the

construct groups, there was a difference between *SOX9/TERT*-PLGA and *SOX9/TERT*-PLGA/fibrin. There was also a significant interaction between weeks and groups, $F(3.00,15.00)=4.21$, $p<0.05$. In the *in vitro* setting, the gene's upregulation pattern was shared with the constructs that were formed using *SOX9/TERT*-transfected chondrocytes, *SOX9/TERT*-PLGA/fibrin, and *SOX9/TERT*-

PLGA (Figure 6(a)). There was a significant difference between each week, $F(1.06,5.31)=36.35$, $p<0.05$. Among the constructs, there was also a significant difference between each group, $F(7=1.60,8.01)=82.55$, $p<0.05$. There was a significant interaction between weeks and groups, $F(1.94,9.71)=38.07$, $p<0.05$.

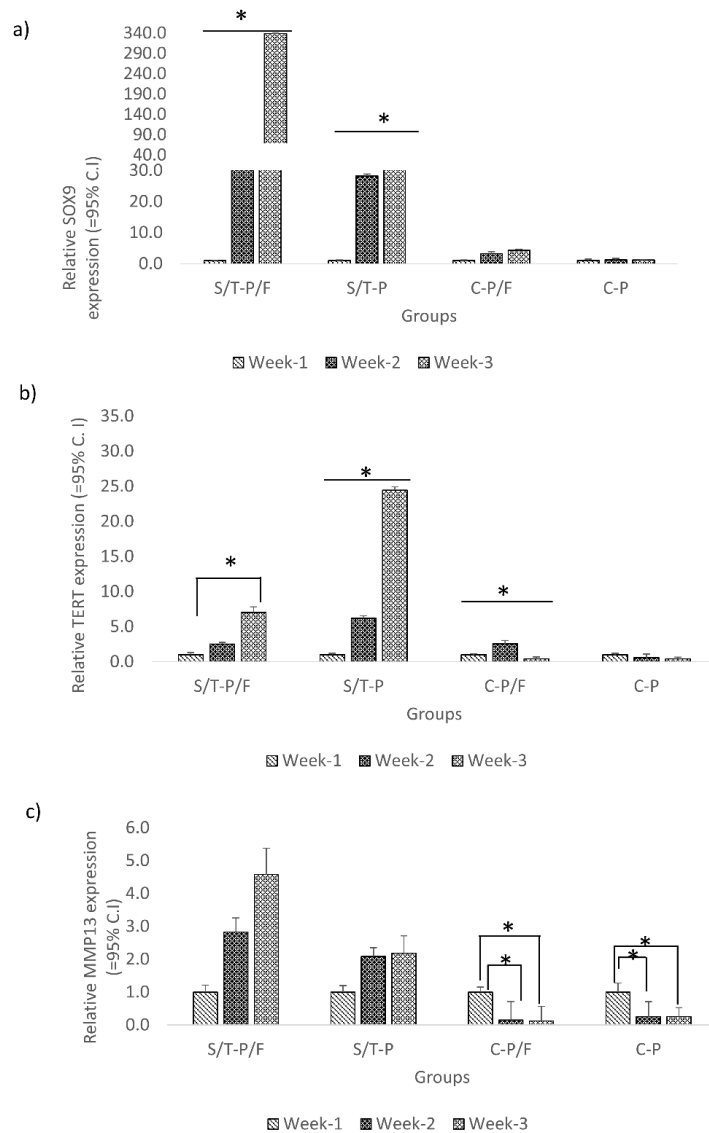


FIGURE 6. a) *SOX9* gene expression was upregulated in the *in vitro* *SOX9/TERT*-PLGA/fibrin and *SOX9/TERT*-PLGA, b) *TERT* gene expression was upregulated in the *in vitro* *SOX9/TERT*-PLGA/fibrin and *SOX9/TERT*-PLG & c) *MMP13* gene expression was upregulated in the *in vitro* *SOX9/TERT*-PLGA/fibrin and *SOX9/TERT*-PLGA. *represents $p < 0.05$ that is considered as significant. The constructs abbreviation is listed in Table 1

In the *in vivo* constructs, *COL1A2* expression was upregulated in *SOX9/TERT*-PLGA/fibrin 3.17-times and 6.38-times in NTC-PLGA (Figure 5(d)), even though the constructs exhibited negative collagen type-I immunoreaction. There was no significant difference between each week, $F(1.00,5.00)=1.69$, $p>0.05$. There was a significant difference between each group, $F(1.70,8.48)=5.73$, $p<0.05$. Among the construct groups, there was a difference between NTC-PLGA and NTC-PLGA/fibrin with *SOX9/TERT*-PLGA. There was also a significant interaction between weeks and groups, $F(1.70,8.48)=5.73$, $p<0.05$. While in the *in vitro* constructs, there were no changes in terms of *COL1A2* expression in *SOX9/TERT*-PLGA/fibrin (Noorhidayah et al. 2019).

As for the *TERT* expression in the *in vivo* constructs, the gene was upregulated in *SOX9/TERT*-PLGA/fibrin by 14.40-times and NTC-PLGA by 3.21-times (Figure 5(e)). There was a significant difference between each week, $F(1.00,5.00)=9.18$, $p>0.05$. There was a significant difference between each group, $F(3.00,15.00)=6.10$, $p<0.05$. Among the construct groups, there was a difference between *SOX9/TERT*-PLGA/fibrin and NTC-PLGA/fibrin with *SOX9/TERT*-PLGA. There was also a significant interaction between weeks and groups, $F(3.00,15.00)=6.10$, $p<0.05$. While in the *in vitro* setting, the gene was upregulated in *SOX9/TERT*-PLGA/fibrin and *SOX9/TERT*-PLGA in the culture. There was no significant difference between each week, $F(1.06,5.32)=5.59$, $p>0.05$. Among the construct groups, there was a significant difference between each group, $F(2.90,14.52)=132.28$, $p<0.05$. There was a significant interaction between weeks and groups, $F(3.11,15.53)=52.28$, $p<0.05$. The regulation of *TERT* in the constructs indicates that the cells have the potential in maintaining its lifespan longer than other constructs because the expressed gene is expected to decelerate the shortening of the telomere sequences during cell division and ultimately delay the apoptosis or senescence of the cells.

The expression of a cartilage-breakdown marker, *MMP13* is also being analysed in both *in vitro* and *in vivo* constructs. *MMP13* targets collagen type-II, proteoglycan, collagen type-IV, collagen type-IX, osteonectin and perlecan which potentially induces arthritis, osteoarthritis and other tissue degrading diseases (Inada et al. 2004; Yamamoto et al. 2016). However, *MMP13* is also involved in embryogenesis, morphogenesis, normal tissue remodelling and tissue repair (Inada et al. 2004; Yamamoto et al. 2016). In the *in vitro* setting, the gene expression was upregulated in *SOX9/TERT*-PLGA/fibrin, and *SOX9/TERT*-PLGA by 4.58-times and 2.18-times, respectively, from week-1 to week-3 (Figure 6(c)). There was a significant difference between each week, $F(2.00,10.00)=114.47$, $p<0.05$. Among the construct groups, there was also a significant difference between each group, $F(7.00,35.00)=61.72$, $p<0.05$. There was a significant interaction between weeks

and groups, $F(14.00,70.00)=53.95$, $p<0.05$. While in the *in vivo* construct, *MMP13* expression was upregulated in *SOX9/TERT*-PLGA/fibrin and NTC-PLGA/fibrin by 2.38-times and 1.29-times, respectively (Figure 5(f)). There was no significant difference between each week, $F(1.00,5.00)=0.18$, $p>0.05$. There was a significant difference between each group, $F(3.00,15.00)=10.61$, $p<0.05$. Among the construct groups, there was a difference between *SOX9/TERT*-PLGA/fibrin and NTC-PLGA with *SOX9/TERT*-PLGA. There was also a significant interaction between weeks and groups, $F(3.00,15.00)=10.61$, $p<0.05$. As supported by the co-expression of the collagens, *MMP13* expression in the constructs was expected as it was also involved in the normal tissue repair and embryonic development. In the overall molecular expression analysis, it has been noted that the *SOX9/TERT*-PLGA/fibrin construct has superior phenotypic expression compared to the other construct groups.

In the previous finding, it has been noted that the synergy of *SOX9* and *TERT* genes facilitates the restoration of cells' phenotype in the 3D culture (Noorhidayah et al. 2019). As a continuation of the work, this study has demonstrated the cartilaginous potential of the implanted constructs that have been formed using *SOX9/TERT*-transfected chondrocytes, in particular the *SOX9/TERT*-PLGA/fibrin construct. The finding has also noted that the genes are able to maintain the cells' chondrogenic phenotype even with one time transfection reaction during monolayer culture (Noorhidayah et al. 2019).

The study has incorporated fibrin with PLGA as it has been proven to soften the inflammatory response, facilitate cell adhesion and proliferation better than PLGA only scaffold (Rozlin et al. 2015). Fibrin seems to accommodate chondrocytes adaptation in the culture medium that may have been affected by the acidic PLGA by-product (Lih et al. 2018). Besides, our previous report has shown that the PLGA/fibrin scaffold promotes better cartilage histoarchitecture than PLGA scaffold *in vitro* (Noorhidayah et al. 2019).

Based on the histology visualisation, it is noted that the *in vivo* environment facilitates tissue growth in stages, where cell proliferation takes place leading to tissue maturation which is confirmed by the concentrated sGAG and proteoglycan at the pericellular matrix region. Nonetheless, a longer implantation period is required to observe tissue maturation (structurally and functionally) or any possible biological effects to the host. It is also suggested to conduct an actual site implantation (orthotopic) assessment on the construct as the tested biological condition is more accurate, and the outcome may differ from ectopic implantation in terms of cells migration and cells' phenotype expression. Further investigation on the *SOX9/TERT*-PLGA/fibrin construct is encouraged because it has the potential to be commercialised as the tissue-engineered product that will contribute to the advancement of organ loss treatment modality.

CONCLUSION

This study demonstrated the cartilage-like tissue formation in the *in vivo* environment. It is noted that the *SOX9/TERT*-PLGA/fibrin construct has exhibited superior phenotypic cartilaginous expression compared to the other construct groups. Through histology, the finding suggested that the cells in the construct had successfully secreted the cartilaginous matrix components. However, the formed tissue is still in its infancy and undergoing a maturation process. The histoarchitecture difference of the constructs in both experimental settings indicates that the *in vivo* setting provides a dynamic environment for complete tissue growth compared to the *in vitro* 3D culture. The extended assessment through orthotopic implantation is necessary in order to obtain in-depth information and understanding of the implanted tissue.

ACKNOWLEDGEMENTS

The authors thanked the Kulliyah of Allied Health Sciences (KAHS), IIUM and Ministry of Science, Technology and Innovation (MOSTI) for providing ScienceFund (SF14-012-0062). The authors also thanked the research team members, KAHS, Dr. Tong Chuan He from University of Chicago, USA for pCDNA3-*SOX9* and Dr. Bob Weinberg from Massachusetts Institute of Technology, USA for pBABE-neo-*hTERT*.

REFERENCES

- Alsberg, E., Anderson, K.W., Albeiruti, A., Rowley, J.A. & Mooney, D.J. 2002. Engineering growing tissues. *Proceedings of the National Academy of Sciences* 99(19): 12025-12030.
- Calabrese, G., Gulino, R., Giuffrida, R., Forte, S., Figallo, E., Fabbi, C., Salvatorelli, L., Memeo, L., Gulisano, M. & Parenti, R. 2017. *In vivo* evaluation of biocompatibility and chondrogenic potential of a cell-free collagen-based scaffold. *Frontiers in Physiology* 8: 984.
- Choi Jiye & Yong Jeong 2017. Elevated emotional contagion in a mouse model of Alzheimer's Disease is associated with increased synchronization in the insula and amygdala. *Scientific Reports* 7: 1-9.
- Deng, Y.H., Lei, G.H., Lin, Z.X., Yang, Y.H., Lin, H. & Tuan, R.S. 2019. Engineering hyaline cartilage from mesenchymal stem cells with low hypertrophy potential *via* modulation of culture conditions and Wnt/ β -catenin pathway. *Biomaterials* 192: 569-578.
- Elakkiya Venugopal, Narmadha Rajeswaran, K. Santosh Sahanand, Amitava Bhattacharyya & Selvakumar Rajendran. 2019. *In vitro* evaluation of phytochemical loaded electrospun gelatin nanofibers for application in bone and cartilage tissue engineering. *Biomedical Materials* 14(1): 015004.
- Inada, M., Wang, Y.M., Byrne, M.H., Rahman, M.U., Miyaura, C., Lopez-Otin, C. & Krane, S.M. 2004. Critical roles for collagenase-3 (Mmp13) in development of growth plate cartilage and in endochondral ossification. *Proceedings of the National Academy of Sciences* 101(49): 17192-17197.
- Karlsson, M. & Björnsson, S. 2001. Quantitation of proteoglycans in biological fluids using Alcian Blue. In *Methods in Molecular Biology*, edited by Lozzo, R.V. Totowa, NJ: Prote. Humana Press Inc.
- Kavand, H., Van Lintel, H. & Renaud, P. 2019. Efficacy of pulsed electromagnetic fields and electromagnetic fields tuned to the ion cyclotron resonance frequency of Ca²⁺ on chondrogenic differentiation. *Journal of Tissue Engineering and Regenerative Medicine* 13(5): 799-811.
- Kudva, A.K., Luyten, F.P. & Patterson, J. 2018. *In vitro* screening of molecularly engineered polyethylene glycol hydrogels for cartilage tissue engineering using periosteum-derived and ATDC5 cells. *International Journal of Molecular Sciences* 19(11): 3341.
- Joydip Kundu, Shim, J.H., Jang, J.N., Kim, S.W. & Cho, D.W. 2013. An additive manufacturing-based PCL-Alginate-chondrocyte bioprinted scaffold for cartilage tissue engineering. *Journal of Tissue Engineering and Regenerative Medicine* 9(11): 1286-1297.
- Lih, E., Kum, C.H., Park, W.R., Chun, S.Y., Cho, Y.J., Joung, Y.K. & Park, K.S. 2018. Modified magnesium hydroxide nanoparticles inhibit the inflammatory response to biodegradable poly(lactide-co-glycolide) implants. *ACS Nano*. 12(7): 6917-6925.
- Liu, Y., Tian, K., Hao, J., Yang, T., Geng, X.L. & Zhang, W.G. 2019. Biomimetic poly (glycerol sebacate)/polycaprolactone blend scaffolds for cartilage tissue engineering. *Journal of Materials Science: Materials in Medicine* 30(5): 53.
- Mohd Yunus Mohd Heikal, Shuid Ahmad Nazrun, Kien Hui Chua & Abd Ghafar Norzana. 2019. *Stichopus chloronotus* aqueous extract as a chondroprotective agent for human chondrocytes isolated from osteoarthritis articular cartilage *in vitro*. *Cytotechnology* 71(2): 521-537.
- Munirah Sha'ban, Ruszymah, Hj Idrus, Samsudin Osman Cassim, Badrul, A.H.M.Y., Azmi Baharudin & Aminuddin Saim. 2008a. Autologous versus pooled human serum for articular chondrocyte growth. *Journal of Orthopaedic Surgery* 16(2): 220-229.
- Munirah Sha'ban, Soon Hee Kim., Ruszymah Hj Idrus & Gilson Khang. 2008b. The use of fibrin and poly(lactic-co-glycolic acid) hybrid scaffold for articular cartilage tissue engineering: An *in vivo* analysis. *European Cells and Materials* 15: 41-52.
- Noorhidayah Md Nazir, Ahmad Hafiz Zulkifly, Kamarul Ariffin Khalid, Ismail Zainol, Zaitunnatakhin Zamli & Munirah Sha'ban. 2019. Matrix production in chondrocytes transfected with sex determining region Y-Box 9 and telomerase reverse transcriptase genes: An *in vitro* evaluation from monolayer culture to three-dimensional culture. *Tissue Engineering and Regenerative Medicine* 16(3): 285-299.
- Ogura, T., Bryant, T., Merkely, G. & Minas, T. 2019. Autologous chondrocyte implantation for bipolar chondral lesions in the patellofemoral compartment: Clinical outcomes at a mean 9 years' follow-up. *American Journal of Sports Medicine* 47(4): 837-846.
- Prosser, A., Scotchford, C., Roberts, G., Grant, D. & Sottile, V. 2019. Integrated multi-assay culture model for stem cell chondrogenic differentiation. *International Journal of Molecular Sciences* 20(4): 951.
- Rozlin Abdul Rahman, Norhamiza Mohamad Sukri, Noorhidayah Md Nazir, Muhammad Aa'zamuddin Ahmad Radzi, Ahmad Hafiz Zulkifly, Aminudin Che Ahmad, Abdurezak Abdulahi Hashi, Suzanah Abdul Rahman & Munirah Sha'ban. 2015. The potential of 3-dimensional construct engineered from

- poly(lactic-co-glycolic acid)/fibrin hybrid scaffold seeded with bone marrow mesenchymal stem cells for *in vitro* cartilage tissue engineering. *Tissue and Cell* 47(4): 420-430.
- Sabatino, M.A., Santoro, R., Gueven, S., Jaquier, C., Wendt, D.J., Martin, I., Moretti, M. & Barbero, A. 2012. Cartilage graft engineering by co-culturing primary human articular chondrocytes with human bone marrow stromal cells. *Pediatric Endocrinology Reviews* 9(12): 1394-1403.
- Sasano, Y., Furusawa, M., Ohtani, H., Mizoguchi, I., Takahashi, I. & Kagayama, M. 1996. Chondrocytes synthesize type I collagen and accumulate the protein in the matrix during development of rat tibial articular cartilage. *Anatomy and Embryology* 194(3): 247-252.
- Schmitz, N., Laverty, S., Kraus, V.B. & Aigner, T. 2010. Basic methods in histopathology of joint tissues. *Osteoarthritis and Cartilage* 18: 113-116.
- Vermeulen, S., Vasilevich, A., Tsiapalis, D., Roumans, N., Vroemen, P., Beijer, N.R.M., Dede-Eren, A., Zeugolis, D. & de Boer, J. 2019. Identification of topographical architectures supporting the phenotype of rat tenocytes. *Acta Biomaterialia* 83: 277-290.
- Wang, T.Y., Lai, J.H., Han, L-H., Tong, X.M. & Yang, F. 2016. Modulating stem cell-Chondrocyte interactions for cartilage repair using combinatorial extracellular matrix-containing hydrogels. *Journal of Materials Chemistry B* 4(47): 7641-7650.
- Yamamoto, K., Okano, H., Miyagawa, W., Visse, R., Shitomi, Y., Santamaria, S., Dudhia, J., Troeberg, L., Strickland, D.K., Hirohata, S. & Nagase, H. 2016. MMP-13 is constitutively produced in human chondrocytes and co-endocytosed with ADAMTS-5 and TIMP-3 by the endocytic receptor LRP1. *Matrix Biology* 56: 57-73.
- Zhang, X.D., Qi, L., Chen, Y.H., Xiong, Z.Z., Li, J.J., Xu, P., Pan, Z.Q., Zhang, H.Z., Chen, Z.X., Xue, K. & Liu, K. 2019. The *in vivo* chondrogenesis of cartilage stem/progenitor cells from auricular cartilage and the perichondrium. *American Journal of Translational Research* 11(5): 2855-2865.
- Zhang, X.W., Wu, S.L., Naccarato, T., Prakash-Damani, M., Chou, Y., Chu, C-Q. & Zhu, Y. 2017. Regeneration of hyaline-like cartilage *in situ* with SOX9 stimulation of bone marrow-derived mesenchymal stem cells. *PLoS ONE* 12(6): e0180138.
- Zhu, Y.Q., Zhang, Y.Y., Yu, L., Tao, R., Xia, H.T., Zheng, R., Shi, Y., Tang, S.J., W.J., Zhang., Liu, W., Cao, Y.L. & Zhou, G.D. 2014. Influence of *Chm-1* knockout on ectopic cartilage regeneration and homeostasis maintenance. *Tissue Engineering Part A* 21(3-4): 782-792.
- Noorhidayah Md Nazir & Zaitunnatakhin Zamli
Department of Biomedical Science
Kulliyah of Allied Health Sciences
International Islamic University Malaysia (IIUM)
Jalan Sultan Ahmad Shah, Bandar Indera Mahkota
25200 Kuantan, Pahang Darul Makmur
Malaysia
- Ahmad Hafiz Zulkifly & Kamarul Ariffin Khalid
Department of Orthopaedics
Traumatology and Rehabilitation
Kulliyah of Medicine
International Islamic University Malaysia (IIUM)
Jalan Hospital Campus
25100 Kuantan, Pahang Darul Makmur
Malaysia
- Ismail Zainol
Department of Chemistry
Faculty of Science and Mathematics
Universiti Pendidikan Sultan Idris (UPSI)
35900 Tanjong Malim, Perak Darul Ridzuan
Malaysia
- Munirah Sha'ban*
Department of Physical Rehabilitation Sciences
Kulliyah of Allied Health Sciences
International Islamic University Malaysia (IIUM)
Jalan Sultan Ahmad Shah, Bandar Indera Mahkota
25200 Kuantan, Pahang Darul Makmur
Malaysia

*Corresponding author; email: munirahshaban@iium.edu.my

Received: 29 July 2019

Accepted: 29 January 2020